Environmental Pollution 370 (2025) 125885

Contents lists available at ScienceDirect

Environmental Pollution

journal homepage: www.elsevier.com/locate/envpol

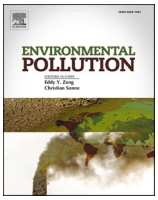

Unveiling novel chloramination byproducts of parabens: Electrophilic coupling mechanisms and their elevated health risks☆

Jialing Luo [a,b], Suling Wei [a,b], Yufeng Xie [a,b], Junlang Qiu [c], Xiaolin Niu [a,b], Na Luo [a,b], Yanpeng Gao [a,b,*], Yuemeng Ji [a,b], Taicheng An [a,b]

[a] Guangdong-Hong Kong-Macao Joint Laboratory for Contaminants Exposure and Health, Guangdong Key Laboratory of Environmental Catalysis and Health Risk Control, Institute Environmental Health and Pollution Control, Guangdong University of Technology, Guangzhou, 510006, China
[b] Guangdong Basic Research Center of Excellence for Ecological Security and Green Development, Key Laboratory of City Cluster Environmental Safety and Green Development of the Ministry of Education, School of Environmental Science and Engineering, Guangdong University of Technology, Guangzhou, 510006, China
[c] Guangdong Provincial Key Laboratory of Environmental Pollution Control and Remediation Technology, School of Environmental Science and Engineering, Sun Yat-sen University, Guangzhou, Guangdong, 510006, China

ARTICLE INFO

Keywords:
Aromatic disinfection byproducts
Chloramination
Methylparaben
Formation mechanism
Coupling DBPs
Health risk

ABSTRACT

The widespread use of chloramination as a disinfection strategy has raised concerns about the formation of harmful disinfection byproducts (DBPs), highlighting the urgent need to elucidate the underlying transformation mechanisms. In this study, we integrated non-targeted screening, organic synthesis, and quantum chemical calculations to investigate the chloramination mechanism of preservative methylparaben and assess the toxicological impacts of the resulting DBPs. In addition to chlorinated products, two novel transformation products, the coupled (C-MeP) and hydroxylated (OH-MeP) products were identified, and the structure of C-MeP was confirmed through synthesized standards. Quantum chemical calculations reveal that the formation of C-MeP is driven by electron transfer, generating radicals that promote C-C bond coupling, while OH-MeP is likely formed by an addition-hydrolysis pathway. The formation of chlorinated products occurs through electrophilic substitution, facilitated by water molecules, and may undergo coupling to form chlorinated products with a biphenyl structure. Toxicity assessments indicate that coupled products exhibit greater negative effects on the gastrointestinal and cardiovascular system compared to parent pollutant. These findings highlight the need to expand the focus of chloramination disinfection beyond traditional chlorinated DBPs, emphasizing the ecological and health implications of novel products including coupled byproducts.

1. Introduction

Disinfection of drinking water is paramount for the prevention of waterborne diseases, playing a crucial role in protecting public health by diminishing exposure to pathogenic microorganisms and reducing the risk of both endemic and epidemic outbreaks. However, the inevitable formation of disinfection by-products (DBPs) poses a significant challenge, as these compounds can introduce serious health risks, e.g., bladder cancer and adverse birth outcomes (Kalita et al., 2024; Li and Mitch, 2018; Xie et al., 2024). Although chloramination can significantly reduce the formation of regulated DBPs such as trihalomethanes (THMs) and haloacetic acids (HAAs) (Hua and Reckhow, 2007), it has been associated with an increased formation of certain unregulated DBPs, such as N-nitrosodimethylamine (NDMA) and various haloaromatic DBPs (Furst et al., 2018; Song et al., 2024; Zhai et al., 2014; Zhang et al., 2022). Notably, some unregulated DBPs exhibit significantly higher cytotoxicity and genotoxicity compared to regulated DBPs (Allen et al., 2022; Liberatore et al., 2017). For instance, certain aromatic DBPs, such as halobenzoquinones and halophenols, exhibit toxicity that is tens to hundreds of times greater than that of THMs (Zhang et al., 2020). Additionally, the developmental toxicity of aromatic DBPs is approximately 50 times greater than that of aliphatic DBPs (Wu et al., 2022). Consequently, increasing attention is being devoted to understanding the formation of these unregulated aromatic DBPs and

☆ This paper has been recommended for acceptance by Ying-Hsuan Lin.

* Corresponding author. Guangdong-Hong Kong-Macao Joint Laboratory for Contaminants Exposure and Health, Guangdong Key Laboratory of Environmental Catalysis and Health Risk Control, Institute Environmental Health and Pollution Control, Guangdong University of Technology, Guangzhou, 510006, China.
E-mail address: gaoyp2016@gdut.edu.cn (Y. Gao).

https://doi.org/10.1016/j.envpol.2025.125885
Received 28 November 2024; Received in revised form 13 January 2025; Accepted 17 February 2025
Available online 18 February 2025

their potential adverse effects on human health.

The pronounced toxicity of aromatic DBPs poses a significant public health risk. Moreover, emerging contaminants in water have become a significant concern due to their potential to form harmful disinfection by-products (DBPs) during chloramination processes. For instance, the ultraviolet filter 2-hydroxy-4-methoxy-5-sulfonic acid benzophenone (BP-4) has been shown to undergo transformation during chloramination, leading to the production of aniline and benzophenone derivatives, which are more toxic and persistent than the parent compound (Sun et al., 2024). Similarly, iodinated DBPs like 4-iodophenol can react with monochloramine to form compounds such as 2,4,6-triiodophenol and 2,6-diiodo-4-nitrophenol, which exhibit higher cytotoxicity (Gong et al., 2017). While these studies have identified potential structures of the newly formed DBPs, the absence of standard reference compounds and the inherent complexity of transformation processes make it challenging to accurately predict reaction pathways, leaving the underlying mechanisms largely unresolved. Moreover, the potential risks posed by these emerging DBPs to both human health and the environment emphasize the urgent need for deeper investigation into their formation mechanisms and associated impacts.

Current research on chloramination mechanisms has primarily focused on the formation of nitrogenous disinfection byproducts (N-DBPs). For example, quantum chemical calculations have revealed that phenylalanine is more likely to form dichloroacetonitrile (DCAN) through the aldehyde pathway rather than the decarboxylation pathway (Yu et al., 2024). Similarly, tertiary amines can lead to the formation of N-nitrosodimethylamine (NDMA) through a series of reactions, including nucleophilic substitution, oxidation, dehydration, and nitrosation under chloramine treatment (Liu et al., 2014). Iodophenol may be substituted by $–NH_2$ from NH_2Cl through nucleophilic substitution, resulting in the formation of the diiodonitrophenol (Gong et al., 2017). Despite progress in understanding N-DBP formation, the mechanisms underlying the formation of other DBP categories, such as aromatic DBPs, remain unclear. This knowledge gap highlights the need for further research to elucidate these mechanisms and evaluate the potential health risks associated with aromatic DBPs.

Parabens, widely used as antimicrobial preservatives, are frequently detected in aquatic environments (Guo and Kannan, 2013; Soni et al., 2005). Studies have shown that methylparaben (MeP) is frequently detected at significant concentrations in drinking water, wastewater treatment plant, surface water and groundwater (Haman et al., 2015; Liu et al., 2020). For instance, MeP concentration have been reported at 47.2 ng/L in drinking water from Egypt, 211–1002 ng/L in wastewater treatment plant influent in Beijing, China, 25–676 ng/L in the surface water from Japan, and up to 194 ng/L in groundwater in Barcelona, Spain(Li et al., 2015; Radwan et al., 2019; Serra-Roig et al., 2016; Yamamoto et al., 2011). Table S2 summarizes reported MeP concentrations in water. Given its prevalence, MeP serves as a key precursor for aromatic DBP formation during chloramination. This study comprehensively investigated the formation mechanisms of aromatic DBPs during chloramination using both experimental and theoretical approaches. Non-targeted and targeted analysis using high-performance liquid chromatography quadrupole time-of-flight mass spectrometry (HPLC-QTOF-MS) initially identified aromatic DBPs, though detection was limited by the absence of product standards. To overcome this, standards were synthesized for comparison, while quantum chemical calculations elucidated reaction pathways at the molecular level. Computational toxicology further assessed the ecological and human health risks of these aromatic DBPs. This study will provide critical insights into the transformation pathways and potential health risks of emerging contaminants including MeP, in chloramination environments. By elucidating these mechanisms, the research addresses a key knowledge gap in the formation of toxic DBPs, which is essential for assessing the risks posed by disinfection processes in water treatment.

2. Materials and methods

2.1. Chemicals and reagents

The free available chlorine (FAC) stock solution was prepared using 4–4.99% sodium hypochlorite (NaOCl) purchased from Sigma-Aldrich. Methylparaben (MeP) was provided by Tokyo Chemical Industry (Japan) (purity >99%). Methyl 3,4-dihydroxybenzoate was supplied by J&K Scientific (purity >98%). Methyl 3-chloro-4-hydroxybenzoate (purity 98%), Methyl 2-chloro-4-hydroxybenzoate (purity 98%) were obtained by Shanghai Macklin Biochemical Technology. 3,5-dichloro-4-hydroxybenzoate was purchased from Shanghai ZZBIO (Shanghai, China). Potassium phosphate monobasic (KH_2PO_4) (99%) and potassium Phosphate Dibasic (K_2HPO_4) (99%) were obtained from Shanghai Aladdin Biochemical Technology (Shanghai, China). Ascorbic Acid (purity 99%) was purchased from Sigma-Aldrich. Optima LC/MS grade water, methanol (MeOH), acetonitrile (ACN), and formic acid (FA, 98% in water) for mass spectrometry were purchased from Sigma-Aldrich. All solutions were prepared using reagent-grade chemicals dissolved in ultrapure water (18.2 MΩ cm) obtained from a Milli-Q system (Millipore).

2.2. Chloramination of MeP in water

The monochloramine (NH_2Cl) solution needs to be freshly prepared before chloramination, with the preparation steps following previously reported methods (Chen et al., 2015). NaOCl and NH_4Cl were mixed slowly and sodium hydroxide solution to maintain the pH at 8.5. The molar ratio of Cl to N was kept at 0.7:1 to minimize the formation of $NHCl_2$) and to ensure that NH_2Cl dominated. Phosphate buffer (10 mM, pH 8) was used to prepare a 100 μM solution of MeP with a molar ratio of monochloramine reacting with MeP of 2:1. Freshly prepared monochloramine (200 μM) was rapidly added to the MeP solution were mixed in an amber glass vial. Under stirring conditions, 100 μM MeP and 200 μM monochloramine were reacted for 6 h, 12 h, 24 h, and 48 h, respectively. A blank control reaction was conducted using MeP solution in phosphate buffer (10 mM) without adding monochloramine. After the set time intervals, under dark conditions at room temperature, ascorbic acid was added to each reaction solution to quench the reaction by reacting with monochloramine. Chloramine samples entering the mass spectrometry assay are pre-treated with solid phase extraction (SPE), details of which are given in Section S1.

2.3. Analysis methods for identification of MeP chloramination

The transformation products of MeP were determined using HPLC-QTOF-MS (Agilent G6545B, USA). Approximately 10 μL sample volumes were directly analyzed via an Agilent Eclipse Plus C18 column (2.1 × 100 mm, particle diameter of 1.7 μm) at the 0.15 mL min^{-1} eluent flow rate. The ratio of A: B was maintained at 98:2 for 5 min, changed linearly to 80:20 over 15 min and to 70:30 over 45 min, then maintained at 30:70 for 10 min. Subsequently, the composition was returned to 98:2 over 55 min and maintained at this ratio for 5 min. The electrospray ionization (ESI) mass spectrometry (MS) in the negative ion mode was operated with a fragment or voltage of 175 V, with argon acting as a collision gas with various collision energies for the analysis of daughter ions.

2.4. Quantum chemistry methods

The structures of MeP and related compounds involved in its chloramination were optimized using the Gaussian 09 software (M. J. Frisch, 2016), with water selected as the solvent model. Density Functional Theory (DFT) was employed for the calculations, and the hybrid M06-2X method with the 6-311G(d,p) basis set was used. At the same level, theoretical harmonic frequencies were calculated to confirm stationary points (no imaginary frequencies) or transition states (TS, with one and

only one imaginary frequency). Intrinsic reaction coordinate (IRC) calculations were performed to connect each TS to its corresponding reactants (RC) and products (PC). Based on these optimized structures, single-point energy calculations were carried out to establish the potential energy surface (PES) at the M06-2X/6–311^{++}G(3df, 2p) level. Additionally, Fukui functions based on DFT were computed to predict reactive sites within the MeP molecule. The Fukui function of MeP and the electron spin density of MeP radicals were calculated using Multiwfn and VMD software (Lu and Chen, 2011).

2.5. Health effect assessment

The ACD/Labs percepta platform provides comprehensive health effects assessments to predict the potential toxicity of pollutants to specific organs and biological systems. The human health impact module is designed to assess the potential organ-specific toxicity of various test compounds by providing probabilistic assessments. Its predictions are based on an extensive dataset encompassing over 100,000 compounds, derived from diverse toxicity studies, including chronic, subchronic, acute, and carcinogenicity assessments (Frydrych and Jurowski, 2024). In this study, the identified transformation products were input into the platform, which then compared their molecular structures with compounds in its database and selected structural analogs to estimate potential health effects. Using QSAR models, the platform evaluates the probability of biological damage or organ injury caused by the compound, particularly its effects on important organs such as the liver, kidney, blood, lungs, cardiovascular system, and gastrointestinal system. By assessing the physicochemical, absorption, distribution, metabolism, and excretion (ADME) properties of compounds, the platform can predict the overall risk that exogenous substances may pose to human health, such as minoxidil, 1-chlordecone, and brominated flame retardants (Cao et al., 2022; Frydrych and Jurowski, 2024; Wang et al., 2021).

3. Results and discussion

3.1. Identification of aromatic disinfection byproducts

Fig. 1 displays the total ion chromatogram (TICs) of the MeP chloramination solution and the control solution (without chloramination) at various reaction times. A comparative analysis of the MS data (*m/z* 50–1500) between the chloraminated and control samples revealed the appearance of six new peaks (peaks P1-P6) in the chloraminated solution, as determined by HPLC-QTOF-MS. Table 1 summarizes the *m/z* values, retention times (RT), predicted molecular formula, and the corresponding mass errors of the six DBPs identified after 48 h of chloramination, as well as their confidence levels according to the Schymanski scale (Schymanski et al., 2014). Determining the precise mass number of the detected product helps to predict its molecular formula. The difference between the theoretical and measured molecular weights of the products was less than 10 ppm, supporting their preliminary identification (Jiang et al., 2021).

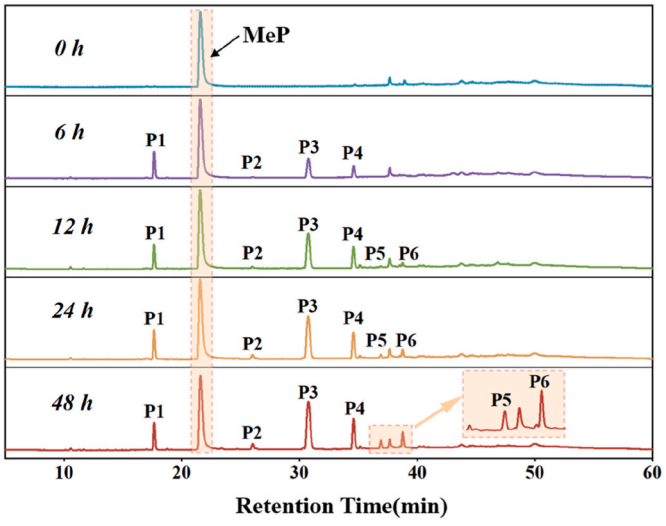

Fig. 1. Total ion current chromatograms (TICs) of MeP chloramination and control solution without chloramination at various reaction times.

Firstly, a new peak P1 was observed prior to the appearance of MeP, with a retention time of 17.67 min (Fig. 1). This indicates that P1 is likely a product with relatively high hydrophilicity. The tentative identification of P1 is presented in Fig. 2a, including the extracted ion chromatogram (XIC), mass spectrum (MS), and tandem mass spectrum (MS/MS). The deprotonated molecular ion of P1 (*m/z* 167.0364) allowed the prediction of its molecular formula as $C_8H_8O_4$, consistent with methyl 3,4-dihydroxybenzoate (OH-MeP). Subsequently, as depicted in Fig. 2a, the RT, mass spectrum, and MS/MS spectrum of P1 were in agreement with those of the OH-MeP standard, confirming the identity of P1 as methyl 3,4-dihydroxybenzoate (OH-MeP). In addition, a newly observed peak pair, P2, with *m/z* values of 200.9962 and 202.9934, exhibited a mass difference of approximately 34 and 36 Da compared to P1 (*m/z* 167.0364) (Fig. S1), suggesting the incorporation of a chlorine atom into the P1 structure. The intensity ratio of the *m/z* 200.9962/202.9932 peaks (100:30) further aligns with the expected isotopic distribution of $^{35}Cl/^{37}Cl$. Accordingly, P2 is a chlorinated product of OH-MeP (Cl-OH-MeP).

Peak P3 exhibited a deprotonated molecular mass of 185.0011/186.9980, approximately 34/36 Da higher than MeP([M-H]$^-$, *m/z* 151.0463), indicating the addition of a chlorine atom to the MeP structure (Fig. S2). The MS spectra matched the calculated mass of chlorinated MeP ([$C_8H_7O_3Cl$-H]$^-$), and the intensity ratio of *m/z* 185.0017/186.9983 (100:33) was consistent with the isotopic pattern of $^{35}Cl/^{37}Cl$, suggesting that P3 is the monochlorinated derivative of MeP. Furthermore, P3 was confirmed as Methyl 3-chloro-4-hydroxybenzoate (Cl-MeP) through a comparative analysis of its RT, MS, and MS/MS spectrum with those of the standard (Fig. S2). Similarly, P5 was identified as methyl 3,5-dichloro-4-hydroxybenzoate (Cl_2-MeP) (Fig. S3). The details are presented in Section S2 of Supplementary Materials.

Interestingly, the *m/z* of the peak P4 was determined as 301.0736, approximately double that of the precursor MeP ([M-H]$^-$ *m/z* 151.0463). Detailed analysis of the MS/MS spectra (Fig. 2b) revealed fragment ions of 242.0578 ([M-H-$COOCH_3$]$^-$) and 185.0594 ([M-H- $COOCH_3$*2]$^-$). These results strongly indicate that the peak P4 is likely a dimer formed by coupling the two MeP molecules. Given the absence of commercially available standards for the MeP dimers, we have synthesized pure C-C and C-O bond-coupled MeP through organic synthesis (Fig. S4a) and confirmed the purity of the synthesized compounds via nuclear magnetic resonance (NMR) spectroscopy (Fig. S4b). Based on the RT, MS and MS/MS spectra of the peak P4 in comparison to the standard sample (Fig. 2b), P4 was confirmed as a dimer formed by the coupling of MeP via C-C bonding (C-MeP), specifically identified as ((2′,6-dihydroxy-5'-((methoxycarbonyl)-[1,1′-bidiphenyl]-3-carbonyl) oxidation) methanide. Furthermore, compared to P4, an increase of 34 Da was observed in peak P6 at *m/z* 335.0330, indicating the addition of a chlorine atom to the P4 structure (Fig. S5). Thus, P6 is a chlorinated C-MeP dimer (Cl-C-MeP). Notably, the identification of both coupling and chlorinated coupling in MeP transformation products during chloramine disinfection is reported for the first time in this study.

In summary, the six aromatic DBPs can be divided into three principal categories: coupling products (C-MeP), hydroxylation products (OH-MeP) and chlorination products (Cl-MeP). Notably, the occurrence of hydroxylation and coupling products in chloramine disinfection systems is infrequently documented, and their formation mechanisms remain poorly understood. To address this gap, we employed quantum chemistry theoretical calculations to investigate the formation

Table 1
Unknown products were detected by nontargeted analysis for MeP treated with chloramination.

#	Exact Mass	Retention Time (min)	Predicted Molecular Formula	Mass Error (ppm)	Confidential Level
P 1	167.0364	17.67	$[C_8H_8O_4\text{-}H]^-$	8.38	Level 1
P 2	200.9962	26.04	$[C_8H_7O_4Cl\text{-}H]^-$	1.00	Level 3
P 3	185.0011	30.73	$[C_8H_7O_3Cl\text{-}H]^-$	0.00	Level 1
P 4	301.0736	34.59	$[C_{16}H_{14}O_6\text{-}H]^-$	0.00	Level 1
P 5	218.9621	36.93	$[C_8H_6O_3Cl_2\text{-}H]^-$	5.98	Level 1
P 6	335.0330	38.79	$[C_{16}H_{13}O_6Cl\text{-}H]^-$	0.60	Level 3

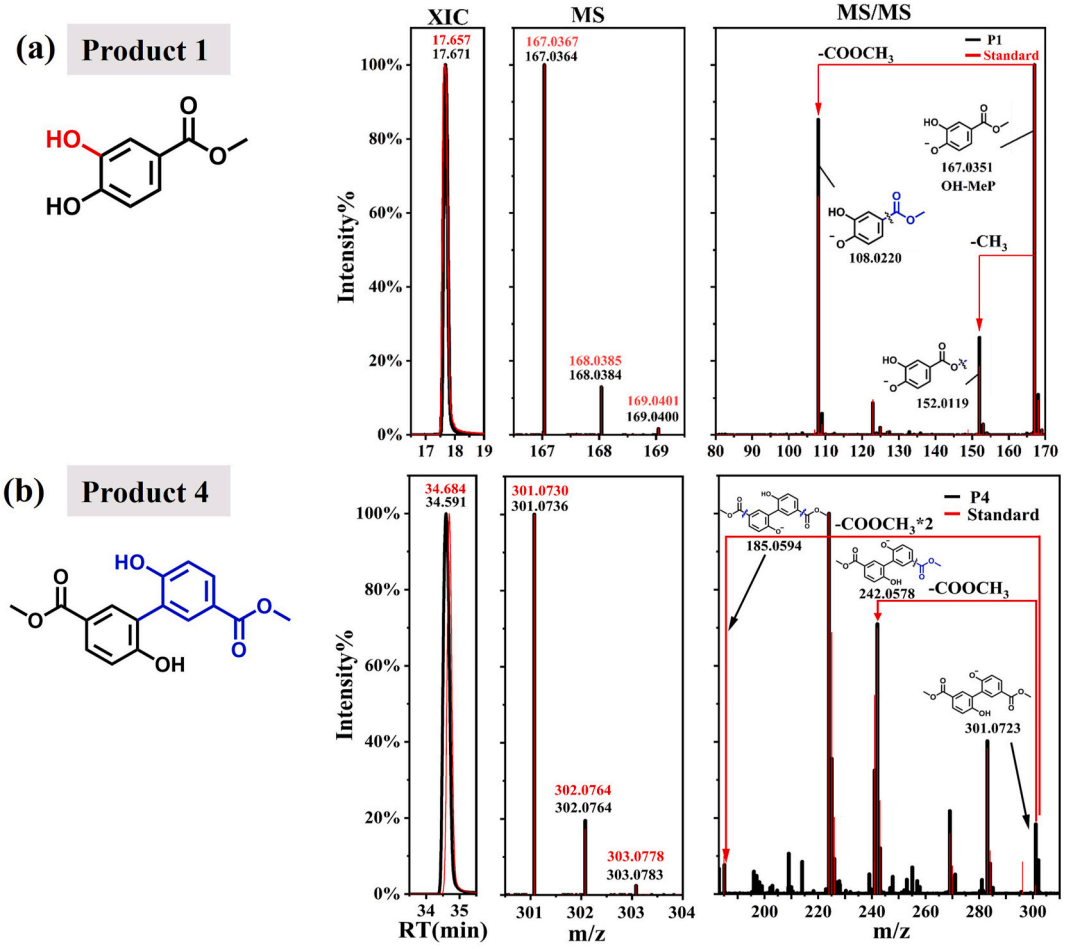

Fig. 2. Extracted Ion Chromatogram (XIC), Mass Spectrum (MS), and Tandem Mass Spectrum (MS/MS) of Unknown Compound P1 (a)/P4 (b) (black line) and Standard (red line). (For interpretation of the references to color in this figure legend, the reader is referred to the Web version of this article.)

mechanisms of these three types of aromatic DBPs. This approach aims to provide a comprehensive understanding of the reaction pathways leading to these novel chlorinated by-products in the chloramine disinfection process.

3.2. Formation mechanisms of aromatic disinfection by-products

3.2.1. Coupling disinfection byproducts

Our research is the first to identify both coupling and chlorinated coupling products derived from MeP during the chloramination process, while the specific formation mechanism remains unclear. Based on the previous research into enzyme-catalyzed reactions of phenolic compounds (Guo et al., 2020; Huang and Weber, 2005), it has been proposed that coupling reactions occur via a single-electron transfer pathway involving phenoxyl radicals generated (Xiang et al., 2020). Given the crucial role of phenoxy radical intermediates in the formation of coupled DBPs, it is hypothesized that alkaline conditions during the chloramination of phenolic compounds are particularly favorable for their generation (Wang et al., 2024). Inspired by the studies, we further investigated the formation mechanisms of coupled DBPs during chloramination of MeP.

Firstly, the speciation of MeP is influenced by pH, with the neutral (MeP) and anionic (MeP^-) forms predominating in the pH range of 7–10. As illustrated in Fig. S6, the anionic form MeP^- was the predominant species (67.1%), followed by the neutral form MeP (32.9%) under chloramine conditions. Consequently, MeP^- could undergo transformation via a single electron transfer (SET) pathway, overcoming a reaction barrier ($\Delta G^{\#}$) of 26.27 kcal mol^{-1} (Fig. 3a), leading to the formation of phenoxy radical (MeP radical, Fig. S7). MeP radical can subsequently couple via C-C bond formation and this radical-radical reaction is an exothermic pathway with a reaction energy of −43.08 kcal mol^{-1} (Details of the calculations are provided in Section S3 of the supplementary data). These findings indicate that the single electron transfer pathway between MeP^- and chlorine is both

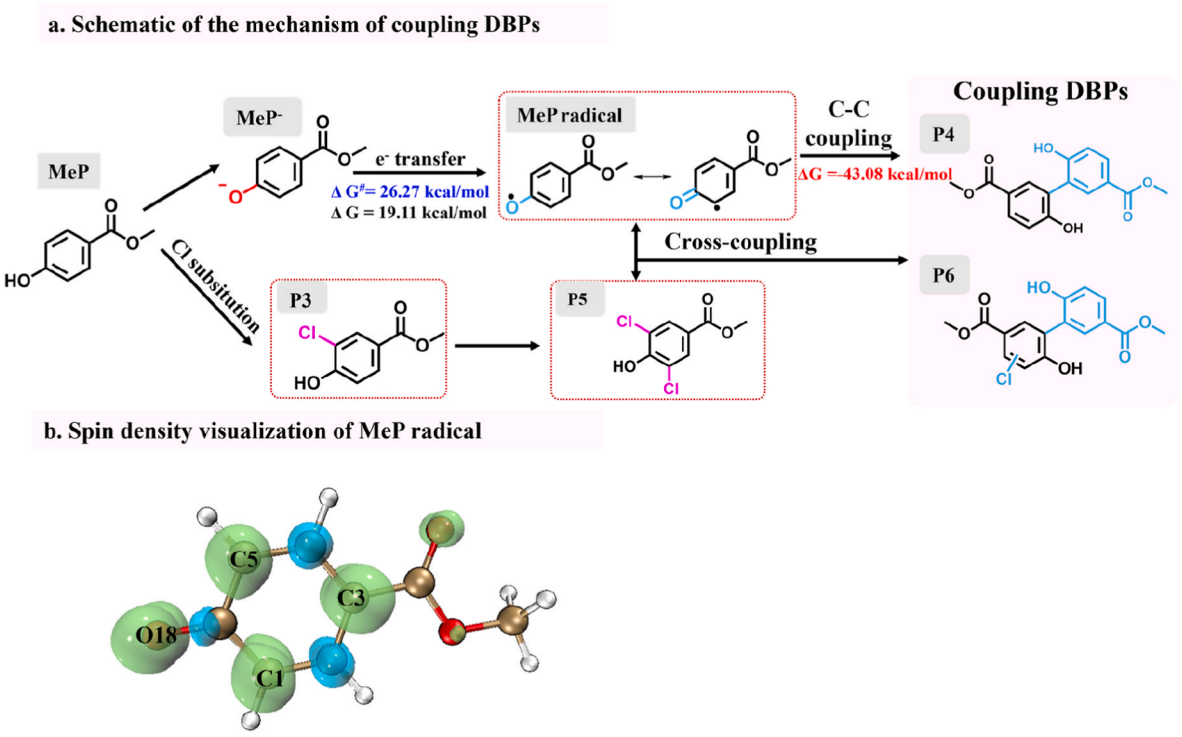

Fig. 3. (a) Reaction mechanism diagram of coupling disinfection by-products (b) Spin density distribution of MeP radical: Positive values are shown in green, negative parts are shown in blue. (For interpretation of the references to color in this figure legend, the reader is referred to the Web version of this article.)

thermodynamically and kinetically favorable, resulting in the generation of coupling products (C-MeP).

Due to the delocalization of the unpaired electron, the phenoxy radical can react with various molecules or radicals at multiple positions during the reaction process. This property facilitates bonding reactions at diverse carbon sites, resulting in a diversity of bonding configurations within the polymer or coupling product. Consequently, elucidating the active sites for covalent bond formation in MeP radicals is essential for understanding the regioselectivity of MeP reactions at different sites and clarifying its coupling reaction pathways. Moreover, the spin distribution of unpaired electrons in free radicals has been shown to affect the regioselectivity of coupling reactions, underscoring the importance of the electron transfer pathway in the reaction mechanism (Elder et al., 2020; Sangha et al., 2012). The sites of free radical reactions are typically localized in areas of elevated spin density, suggesting that covalent bond formation is more probable in these regions. Therefore, we calculate the spin density and spin population of MeP radical (detailed explanation in Section S4). The calculated spin density of each atom in the MeP radical is presented in Table S1 and Fig. 3b. Due to high spin densities, the unpaired electrons are more likely to be concentrated on the hydroxyl oxygen (O18) and its adjacent carbon atoms (C1 and C5) as well as the para-carbon atom (C3) of the MeP benzene ring. Although the carbon and oxygen atoms in the para position of the ester group also exhibit relatively high spin densities, these positions are less likely to serve as favorable sites for MeP coupling reactions because of steric hindrance effects. Consequently, the most reactive bonding sites in the MeP radical are mainly concentrated on the hydroxyl oxygen and neighboring carbon atoms, facilitating the coupling reaction. This calculation is validated with our experimental observation of structures generated on the C-C bond coupler (C-MeP) adjacent to the phenolic hydroxybenzene ring of MeP. Similarly, a coupling reaction can occur between MeP and its chlorination product (Fig. 3a), resulting in the formation of chlorinated C-MeP (Cl-C-MeP).

3.2.2. *Chlorination disinfection byproducts*

To facilitate the rapid prediction of potential active reaction sites for MeP, we computed the condensed Fukui functions (CFF) of MeP molecules using DFT, as detailed in Section S5. The calculated condensed Fukui (f^+, f^-, f^0, Δf) values are illustrated in Fig. S8. The phenolic hydroxyl group (O10) of MeP exhibited the highest f^0 value (0.0972), indicating a strong tendency to participate in free radical reactions. Furthermore, the hydroxy oxygen (O10) and the ortho and para-carbon atoms (C1, C3, and C5) showed a high reactivity towards electrophilic reactions, with their low Δf values of −0.0944, −0.0488, −0.0548, and −0.0432, respectively. Considering steric effects, the ortho position of the -OH group in MeP is more prone to electrophilic attack by chloramine than the para position. This theoretical prediction is corroborated by our chloramination experiments, which identified mono- and dichlorinated products at the ortho position of the -OH group. Furthermore, to gain deeper insights into the formation mechanisms of these disinfection by-products (DBPs), we performed quantum chemical calculations focusing on the ortho-carbon sites adjacent to the hydroxyl group in MeP.

We initially examined the potential pathways for MeP chlorination by NH_2Cl, focusing on Cl-atom attack (R_A) mechanisms. Fig. 4 illustrates the free energy surfaces of the R_A route, which were obtained after full optimization of all related intermediates, transition states, and products (Details of the definitions are described in Section S6). The R_A route involves the direct Cl-substitution of MeP by NH_2Cl via a single concerted transition state (TS_A)[NH_2Cl•••MeP], with a reaction barrier ($\Delta G^{\#}$) of 92.78 kcal mol^{-1}, leading to the formation of Cl-MeP. This route is an exothermic process with a negative reaction energy (−17.92 kcal mol^{-1}). During this electrophilic substitution, a chlorine atom replaces a hydrogen atom at the adjacent position, resulting in the formation of the monochlorinated product (Cl-MeP). Since the transition energy barrier $\Delta G^{\#}$ of the Cl-atom attack pathway (R_A) reaches 92.78 kcal mol^{-1}, such a high energy barrier indicates that the reaction is energetically unfavorable and unlikely to occur readily. However, chlorinated products are frequently detected in the actual water

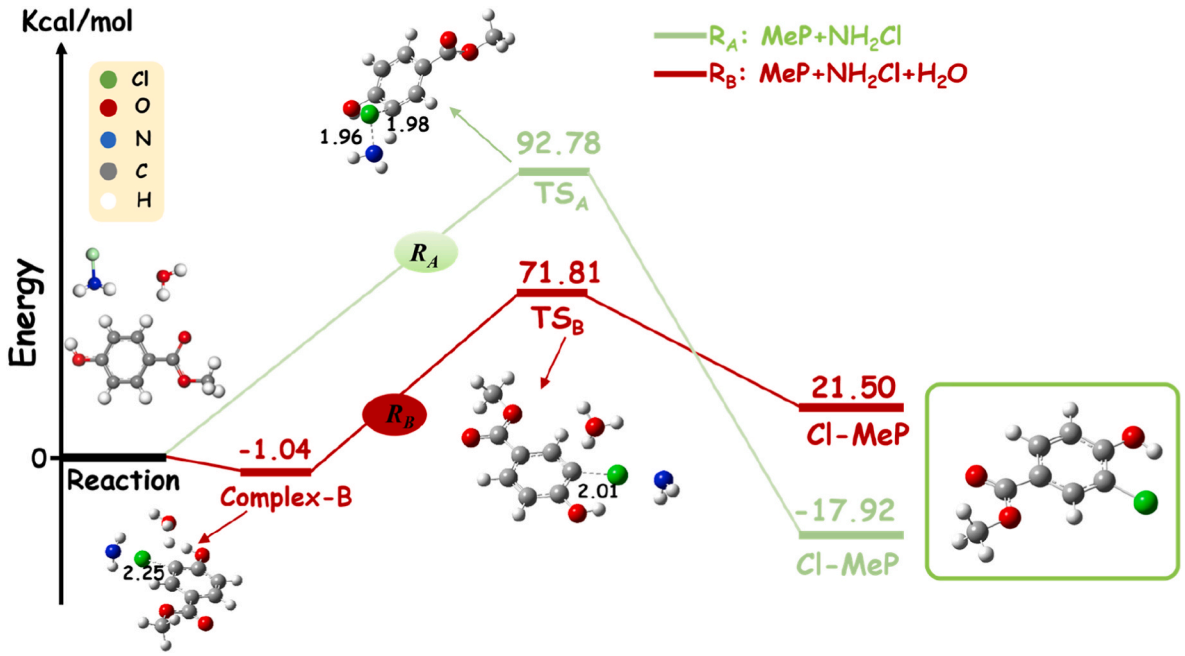

Fig. 4. Free energy surface of MeP reaction with NH_2Cl (energy in kcal·mol^{-1}, bond length in Å).

environment.

To address this apparent contradiction, we further investigated a stepwise reaction mechanism to identify a more feasible pathway for the formation of Cl-MeP. We speculated that a more reactive species might be involved in the chloramination disinfection process of MeP, facilitating the formation of Cl-MeP. Considering the previous research, which demonstrated that H_2O can act as a Brønsted base for the leaving proton, thereby significantly lowering the reaction energy barrier and promoting the formation of iodinated disinfection by-products (I-DBPs) (Gao et al., 2022), we considered a similar role for H_2O in the formation of Cl-MeP. To further explore this, we investigated the R_B pathway, which involves a cooperative reaction of MeP with NH_2Cl in the presence of H_2O). This pathway involves a stepwise reaction mechanism where a complex (Complex) [NH_2Cl•••MeP] is rapidly formed, followed by a rate-determining deprotonation step, ultimately leading to the formation of Cl-MeP. Surprisingly, MeP and NH_2Cl can easily form a loosely bound complex (Complex-B) through a non-energetic process. Subsequently, Cl-MeP is formed via the transition state (TS_B) [NH_2Cl•••MeP•••H_2O] in the presence of H_2O. The barrier for the R_B pathway is 71.81 kcal mol^{-1}, approximately 20.97 kcal mol^{-1} lower than that of the pathway R_A. Our calculations reveal that the stepwise Cl-attack (R_B) is the more favorable route for the formation of Cl-MeP, compared to the direct Cl-substitution pathway.

3.2.3. *Hydroxylation disinfection byproducts*

As shown in Fig. S9, MeP was attacked by an N atom of chloramine, and NH_2-addition to the C atom adjacent to the phenolic hydroxyl group on MeP led to the formation of the amino adduct intermediate (NH_2-MeP) of MeP. The pathway began with the amino(-NH_2) addition of MeP, wherein the nitrogen atom of NH_2Cl connected with the unsubstituted C1 atom on the benzene ring of MeP via the transition state (TS) [Cl(NH_2)•••MeP] with an energy barrier of 40.96 kcal mol^{-1}, forming intermediate (IM-NH_2-MeP). The reaction energy for this process is 7.08 kcal mol^{-1}. OH-MeP can be attributed to the weakly alkaline environment of the chloramination condition, where the solvent water (H_2O) dissociates into a higher concentration of hydroxide ions (OH^-). The transient intermediate NH_2-MeP, due to its instability, leads to the detachment of the amino group. This results in the hydrolysis of MeP, forming the hydroxylated product OH-MeP with the free energy of −17.39 kcal mol^{-1}.

Based on theoretical calculation and the HPLC-QTOF-MS product identification, the transformation pathways of MeP during chloramination disinfection are illustrated in Fig. S10. In summary, the transformation of the parent compound primarily initiates at the carbon atom adjacent to the phenolic hydroxyl group, proceeding through three main pathways: (1) formation of coupling DBPs, C-MeP and Cl-C-MeP; (2) formation of hydroxylated DBPs, OH-MeP and Cl-OH-MeP. (3) formation of chlorinated DBPs, Cl-MeP and Cl_2-MeP. The yields of these major products vary over time, as illustrated in Fig. S11. Prolonged chloramination leads to a significant increase in the yields of chlorinated and coupling products, while the yield of hydroxylated DBPs remains relatively stable. For instance, after 48 h of reaction, the yields of coupling, chlorinated, and hydroxylated products increase by 4.2, 3.5, and 1.3 times, respectively, compared to 6 h. This suggests that while the formation of hydroxylated products stabilizes early, chlorinated and coupling products continue to accumulate, likely due to ongoing chlorination and coupling reactions under extended reaction conditions. These transformation pathways are consistent with the density functional theory calculations of the Fukui index (Fig. S8). Moreover, with prolonged reaction time, electrophilic sites on the MeP phenyl ring may undergo additional chlorination, potentially leading to ring cleavage and the formation of smaller chlorinated DBPs (Nihemaiti et al., 2017). In addition to forming dimers, coupled DBPs may undergo further coupling and polymerization, resulting in the formation of trimers or chlorinated trimers (Li et al., 2022). Structurally, the chlorinated coupling products (Cl-C-MeP) are notably similar to the carcinogenic polychlorinated biphenyls (PCBs), potentially posing significant ecological and human health risks. Currently, research on disinfection processes has predominantly focused on chlorinated compounds, while the environmental and health implications of these coupling products and hydroxylated derivatives have not yet been sufficiently explored. Therefore, comprehensive studies are warranted to thoroughly assess the toxicological impacts of these transformation products.

3.3. *Toxicity assessment of the formed DBPs in chloramination*

Fig. 5 illustrates the toxicological profiles of six transformation products formed in chloramination of MeP. The risk values, ranging

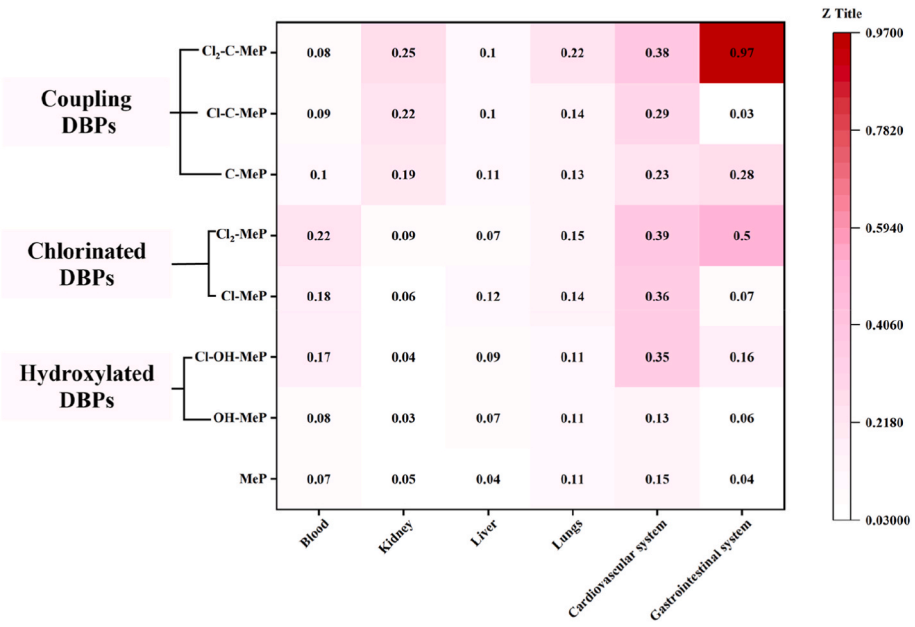

Fig. 5. Computational prediction of DBPs as compared to parent MeP (The redder the color, the more damage the substance can cause to human organs). (For interpretation of the references to color in this figure legend, the reader is referred to the Web version of this article.)

from 0 to 1, reflect the relative potential hazards these transformation products pose to various human physiological systems, with higher values indicating elevated risk. The findings reveal that while OH-MeP displays a modest increase in toxicity to the human digestive system and liver compared to the parent compound MeP, the overall difference in toxicity is minimal. However, it is noteworthy that disinfection by-products with chlorine substitution (Cl-C-MeP, Cl-OH-MeP, Cl-MeP, Cl_2-MeP) exhibit a significant increase in toxicity across various human systems. It is readily observable that the incorporation of chlorine atoms significantly increases the health risk to the blood, cardiovascular system, and gastrointestinal system. The greater the number of chlorine atoms, the more toxic it is to the gastrointestinal system. Among these, Cl_2-MeP shows a significant increase in toxicity to the cardiovascular (0.39) and gastrointestinal (0.5) systems compared to the parent compound MeP (0.15, 0.04, respectively). Notably, the dichlorinated coupling DBPs (Cl_2-C-MeP) exhibit remarkably high toxicity towards the human gastrointestinal systems, with a risk value of 0.97. This elevated toxicity is hypothesized to arise from their structural resemblance to polychlorinated biphenyls (PCBs), which may lead to significant differences in toxicological profiles compared to other transformation products. Furthermore, the coupling DBPs exhibit increased adverse effects on the kidneys, liver, and digestive system relative to the parent compound MeP, underscoring the potential health risks associated with these by-products in chloramination systems. Given these findings, the health implications of coupling DBPs warrant careful consideration. In addition, we evaluated the acute toxicity, bioaccumulation potential, developmental toxicity, and mutagenicity of MeP and its chloramination products on aquatic organisms (Fig. S12). The results indicate that coupling DBPs can impair the growth and development of aquatic organisms and may pose a risk of causing mutations and deformities.

4. Conclusions

During the chloramination process, a range of novel aromatic DBPs are formed, including hydroxylated derivatives (Cl-OH-MeP, OH-MeP), chlorinated products (Cl-MeP, Cl_2-MeP), and coupling products (C-MeP, Cl-C-MeP). This study is the first to structurally characterize these hydroxylated and coupling byproducts using organic synthesis methods, confirmed through high-resolution mass spectrometry (LC-QTOF-MS) and supported by quantum chemical calculations. Furthermore, we have elucidated the chloramination pathways of MeP and the formation of these novel aromatic DBPs. Toxicity assessments indicate that the chlorinated DBPs (Cl-MeP, Cl_2-MeP) and coupling DBPs (C-MeP, Cl-C-MeP, Cl_2-C-MeP) exhibit higher toxicity compared to the parent compound MeP, with adverse effects particularly on the gastrointestinal and cardiovascular systems. Furthermore, these novel aromatic DBPs pose potential certain environmental risks, including acute toxicity, bioaccumulation potential, and mutagenic effects in aquatic organisms. Our findings underscore the importance of considering these previously unrecognized aromatic DBPs in the safety evaluation of chloramination, alongside the routinely monitored trihalomethanes (THMs, 80 μg/L) and haloacetic acids (HAAs, 60 μg/L) regulated by the U.S. Environmental Protection Agency (US EPA) (EPA, 2008). While this study provides valuable insights into the formation mechanisms and toxicity of novel DBPs, we acknowledge the need for further investigations under more realistic conditions (e.g., lower concentrations) to validate the proposed mechanism in practical drinking water systems. Based on our findings, we recommend that future research to focus on optimizing disinfectant dosing and reaction time, enhancing water quality monitoring, and improving post-treatment processes to mitigate the risk of increased water toxicity during disinfection. This study provides new insights into the transformation mechanisms of MeP during chloramination and offers scientific evidence for optimizing water treatment processes and improving water quality safety.

CRediT authorship contribution statement

Jialing Luo: Writing – original draft, Visualization, Validation, Software, Methodology, Investigation, Formal analysis. **Suling Wei:** Visualization, Software, Methodology, Investigation, Formal analysis. **Yufeng Xie:** Visualization, Software, Methodology, Investigation, Formal analysis. **Junlang Qiu:** Validation, Methodology, Investigation. **Xiaolin Niu:** Validation, Methodology. **Na Luo:** Validation, Methodology. **Yanpeng Gao:** Writing – review & editing, Visualization, Validation, Supervision, Software, Methodology, Investigation, Funding acquisition, Data curation, Conceptualization. **Yuemeng Ji:** Conceptualization. **Taicheng An:** Supervision.

Declaration of competing interest

The authors declare that they have no known competing financial interests or personal relationships that could have appeared to influence the work reported in this paper.

Acknowledgments

We thank the National Natural Science Foundation of China (42322704,42277222), Guangdong Basic and Applied Basic Research Foundation (2023B1515020078) and National Key Research and Development Program of China (2022YFC3105600).

Appendix A. Supplementary data

Supplementary data to this article can be found online at https://doi.org/10.1016/j.envpol.2025.125885.

Data availability

Data will be made available on request.

References

Allen, J.M., Plewa, M.J., Wagner, E.D., Wei, X., Bokenkamp, K., Hur, K., Jia, A., Liberatore, H.K., Lee, C.-F.T., Shirkhani, R., Krasner, S.W., Richardson, S.D., 2022. Drivers of disinfection byproduct cytotoxicity in U.S. Drinking water: should other DBPs Be considered for regulation? Environ. Sci. Technol. 56 (1), 392–402.

Cao, Y., Gao, Y., Hu, X., Zeng, Y., Luo, X., Li, G., An, T., Mai, B., 2022. Insight into phototransformation mechanism and toxicity evolution of novel and legacy brominated flame retardants in water: a comparative analysis. Water Res. 211, 118041.

Chen, B., Qian, Y., Wu, M., Zhu, L., Hu, B., Li, X.-F., 2015. Identification of precursors and mechanisms of tobacco-specific nitrosamine formation in water during chloramination. Environ. Sci. Technol. 49 (1), 459–466.

Elder, T., del Río, J.C., Ralph, J., Rencoret, J., Kim, H., Beckham, G.T., Crowley, M.F., 2020. Coupling and reactions of lignols and new lignin monomers: a density functional theory study. ACS Sustain. Chem. Eng. 8 (30), 11033–11045.

EPA, U., 2008. National Primary Drinking Water Regulations. U.S. Environmental Protection Agency, Washington, DC.

M.J. Frisch, G.W.T., H.B. Schlegel, G.E. Scuseria, M.A. Robb, J.R. Cheeseman, G. Scalmani, V. Barone, G.A. Petersson, H. Nakatsuji, X. Li, M. Caricato, A. Marenich, J. Bloino, B.G. Janesko, R. Gomperts, B. Mennucci, H.P. Hratchian, J.V. Ortiz, A.F. Izmaylov, J.L. Sonnenberg, D. Williams-Young, F. Ding, F. Lipparini, F. Egidi, J. Goings, B. Peng, A. Petrone, T. Henderson, D. Ranasinghe, V.G. Zakrzewski, J. Gao, N. Rega, G. Zheng, W. Liang, M. Hada, M. Ehara, K. Toyota, R. Fukuda, J. Hasegawa, M. Ishida, T. Nakajima, Y. Honda, O. Kitao, H. Nakai, T. Vreven, K. Throssell, J.A. Montgomery, Jr., J.E. Peralta, F. Ogliaro, M. Bearpark, J.J. Heyd, E. Brothers, K.N. Kudin, V.N. Staroverov, T. Keith, R. Kobayashi, J. Normand, K. Raghavachari, A. Rendell, J.C. Burant, S.S. Iyengar, J. Tomasi, M. Cossi, J. M. Millam, M. Klene, C. Adamo, R. Cammi, J.W. Ochterski, R.L. Martin, K. Morokuma, O. Farkas, J.B. Foresman, and D.J. Fox, Gaussian, Inc., Wallingford CT, (2016).

Frydrych, A., Jurowski, K., 2024. Toxicity of minoxidil – comprehensive in silico prediction of main toxicity endpoints: acute toxicity, irritation of skin and eye, genetic toxicity, health effect, cardiotoxicity and endocrine system disruption. Chem. Biol. Interact. 393, 110951.

Furst, K.E., Pecson, B.M., Webber, B.D., Mitch, W.A., 2018. Tradeoffs between pathogen inactivation and disinfection byproduct formation during sequential chlorine and chloramine disinfection for wastewater reuse. Water Res. 143, 579–588.

Gao, Y., Qiu, J., Ji, Y., Wawryk, N.J.P., An, T., Li, X.-F., 2022. Formation mechanism of iodinated aromatic disinfection byproducts: acid catalysis with H2OI+. Environ. Sci. Technol. 56 (3), 1791–1800.

Gong, T., Tao, Y., Zhang, X., Hu, S., Yin, J., Xian, Q., Ma, J., Xu, B., 2017. Transformation among aromatic iodinated disinfection byproducts in the presence of monochloramine: from monoiodophenol to triiodophenol and diiodonitrophenol. Environ. Sci. Technol. 51 (18), 10562–10571.

Guo, Y., Kannan, K., 2013. A survey of phthalates and parabens in personal care products from the United States and its implications for human exposure. Environ. Sci. Technol. 47 (24), 14442–14449.

Guo, F., Chai, L., Zhang, S., Yu, H., Liu, W., Kepp, K.P., Ji, L., 2020. Computational biotransformation profile of emerging phenolic pollutants by cytochromes P450: phenol-coupling mechanism. Environ. Sci. Technol. 54 (5), 2902–2912.

Haman, C., Dauchy, X., Rosin, C., Munoz, J.-F., 2015. Occurrence, fate and behavior of parabens in aquatic environments: a review. Water Res. 68, 1–11.

Hua, G., Reckhow, D.A., 2007. Comparison of disinfection byproduct formation from chlorine and alternative disinfectants. Water Res. 41 (8), 1667–1678.

Huang, Q., Weber, W.J., 2005. Transformation and removal of bisphenol A from aqueous phase via peroxidase-mediated oxidative coupling reactions: efficacy, products, and pathways. Environ. Sci. Technol. 39 (16), 6029–6036.

Jiang, P., Qiu, J., Gao, Y., Stefan, M.I., Li, X.-F., 2021. Nontargeted identification and predicted toxicity of new byproducts generated from UV treatment of water containing micropollutant 2-mercaptobenzothiazole. Water Res. 188, 116542.

Kalita, I., Kamilaris, A., Havinga, P., Reva, I., 2024. Assessing the health impact of disinfection byproducts in drinking water. ACS ES&T Water 4 (4), 1564–1578.

Li, X.-F., Mitch, W.A., 2018. Drinking water disinfection byproducts (DBPs) and human health effects: multidisciplinary challenges and opportunities. Environ. Sci. Technol. 52 (4), 1681–1689.

Li, W., Shi, Y., Gao, L., Liu, J., Cai, Y., 2015. Occurrence, fate and risk assessment of parabens and their chlorinated derivatives in an advanced wastewater treatment plant. J. Hazard Mater. 300, 29–38.

Li, W., Zhang, X., Han, J., 2022. Formation of larger molecular weight disinfection byproducts from acetaminophen in chlorine disinfection. Environ. Sci. Technol. 56 (23), 16929–16939.

Liberatore, H.K., Plewa, M.J., Wagner, E.D., VanBriesen, J.M., Burnett, D.B., Cizmas, L. H., Richardson, S.D., 2017. Identification and comparative mammalian cell cytotoxicity of new iodo-phenolic disinfection byproducts in chloraminated oil and gas wastewaters. Environ. Sci. Technol. Lett. 4 (11), 475–480.

Liu, Y.D., Selbes, M., Zeng, C., Zhong, R., Karanfil, T., 2014. Formation mechanism of NDMA from ranitidine, trimethylamine, and other tertiary amines during chloramination: a computational study. Environ. Sci. Technol. 48 (15), 8653–8663.

Liu, Z., Tam, N.F.Y., Kuo, D.T.F., Wu, Q., Du, Y., Shi, Y., Kong, D., Zhang, Y., Li, H., Hu, X., 2020. Removal, seasonal variation, and environmental impact of parabens in a municipal wastewater treatment facility in Guangzhou, China. Environ. Sci. Pollut. Control Ser. 27 (22), 28006–28015.

Lu, T., Chen, F., 2011. Multiwfn: a multifunctional wavefunction analyzer. J. Comput. Chem. 33 (5), 580–592.

Nihemaiti, M., Le Roux, J., Hoppe-Jones, C., Reckhow, D.A., Croué, J.-P., 2017. Formation of haloacetonitriles, haloacetamides, and nitrogenous heterocyclic byproducts by chloramination of phenolic compounds. Environ. Sci. Technol. 51 (1), 655–663.

Radwan, E.K., Ibrahim, M.B.M., Adel, A., Farouk, M., 2019. The occurrence and risk assessment of phenolic endocrine-disrupting chemicals in Egypt's drinking and source water. Environ. Sci. Pollut. Control Ser. 27 (2), 1776–1788.

Sangha, A.K., Parks, J.M., Standaert, R.F., Ziebell, A., Davis, M., Smith, J.C., 2012. Radical coupling reactions in lignin synthesis: a density functional theory study. J. Phys. Chem. B 116 (16), 4760–4768.

Schymanski, E.L., Jeon, J., Gulde, R., Fenner, K., Ruff, M., Singer, H.P., Hollender, J., 2014. Identifying small molecules via high resolution mass spectrometry: communicating confidence. Environ. Sci. Technol. 48 (4), 2097–2098.

Serra-Roig, M.P., Jurado, A., Díaz-Cruz, M.S., Vázquez-Suñé, E., Pujades, E., Barceló, D., 2016. Occurrence, fate and risk assessment of personal care products in river–groundwater interface. Sci. Total Environ. 568, 829–837.

Song, M., Wang, J., DeNicola, M., Hanigan, D., 2024. Natural vs. anthropogenic sources of N-Nitrosodimethylamine precursors in surface water. Water Res. 265, 122313.

Soni, M.G., Carabin, I.G., Burdock, G.A., 2005. Safety assessment of esters of p-hydroxybenzoic acid (parabens). Food Chem. Toxicol. 43 (7), 985–1015.

Sun, X., Wei, D., Wang, F., Yang, F., Du, Y., Xiao, H., Wei, X., Xiao, A., 2024. Formation of nitrogen-containing disinfection by-products during the chloramination treatment of an emerging pollutant. Chemosphere 353, 141536.

Wang, M., Gao, Y., Li, G., An, T., 2021. Increased adverse effects during metabolic transformation of short-chain chlorinated paraffins by cytochrome P450: a theoretical insight into 1-chlorodecane. J. Hazard Mater. 407, 124391.

Wang, P., Ye, B., Nomura, Y., Fujiwara, T., 2024. Revisiting the chloramination of phenolic compounds: formation of novel high-molecular-weight nitrogenous disinfection byproducts. Water Res. 266, 122335.

Wu, Y., Wei, W., Luo, J., Pan, Y., Yang, M., Hua, M., Chu, W., Shuang, C., Li, A., 2022. Comparative toxicity analyses from different endpoints: are new cyclic disinfection byproducts (DBPs) more toxic than common aliphatic DBPs? Environ. Sci. Technol. 56 (1), 194–207.

Xiang, W., Qu, R., Wang, X., Wang, Z., Bin-Jumah, M., Allam, A.A., Zhu, F., Huo, Z., 2020. Removal of 4-chlorophenol, bisphenol A and nonylphenol mixtures by aqueous chlorination and formation of coupling products. Chem. Eng. J. 402, 126140.

Xie, Z., Guan, J., Lei, X., Fan, M., Qiu, J., Yang, X., 2024. Advances in toxicity assessment of drinking water disinfection byproducts. TrAC, Trends Anal. Chem. 172, 117545.

Yamamoto, H., Tamura, I., Hirata, Y., Kato, J., Kagota, K., Katsuki, S., Yamamoto, A., Kagami, Y., Tatarazako, N., 2011. Aquatic toxicity and ecological risk assessment of seven parabens: individual and additive approach. Sci. Total Environ. 410–411, 102–111.

Yu, R., Qian, Y., Chen, Y., Shi, Y., Guo, J., An, D., 2024. Computational-aided analysis of the pathway and mechanism of dichloroacetonitrile formation from phenylalanine upon chloramination. Sci. Total Environ. 926, 171995.

Zhai, H., Zhang, X., Zhu, X., Liu, J., Ji, M., 2014. Formation of brominated disinfection byproducts during chloramination of drinking water: new polar species and overall kinetics. Environ. Sci. Technol. 48 (5), 2579–2588.

Zhang, Z.X., Zhu, Q.Y., Huang, C., Yang, M.T., Li, J.Y., Chen, Y.T., Yang, B., Zhao, X., 2020. Comparative cytotoxicity of halogenated aromatic DBPs and implications of the corresponding developed QSAR model to toxicity mechanisms of those DBPs: binding interactions between aromatic DBPs and catalase play an important role. Water Res. 170, 115283.

Zhang, D., Bond, T., Pan, Y., Li, M., Luo, J., Xiao, R., Chu, W., 2022. Identification, occurrence, and cytotoxicity of haloanilines: a new class of aromatic nitrogenous disinfection byproducts in chloraminated and chlorinated drinking water. Environ. Sci. Technol. 56 (7), 4132–4141.